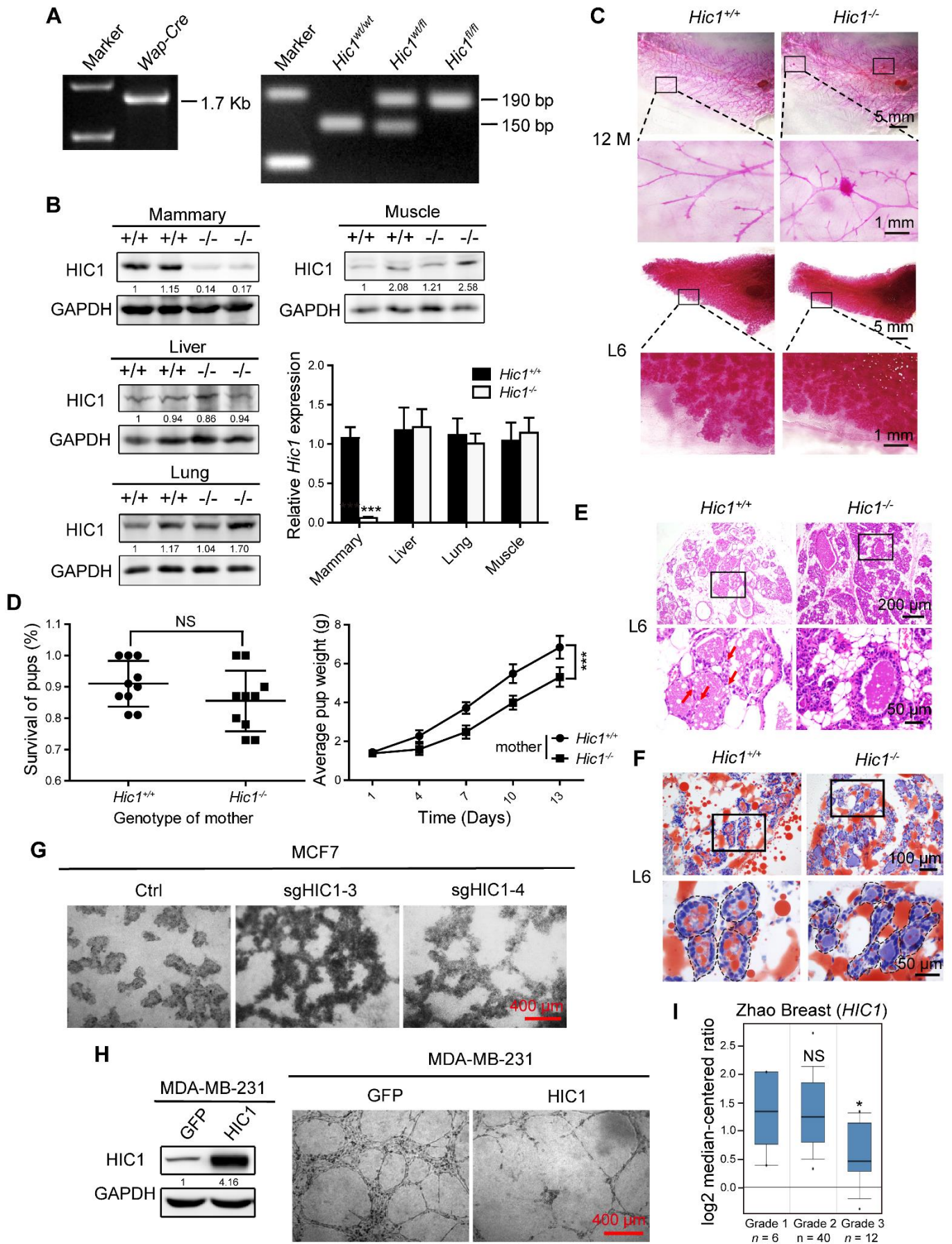
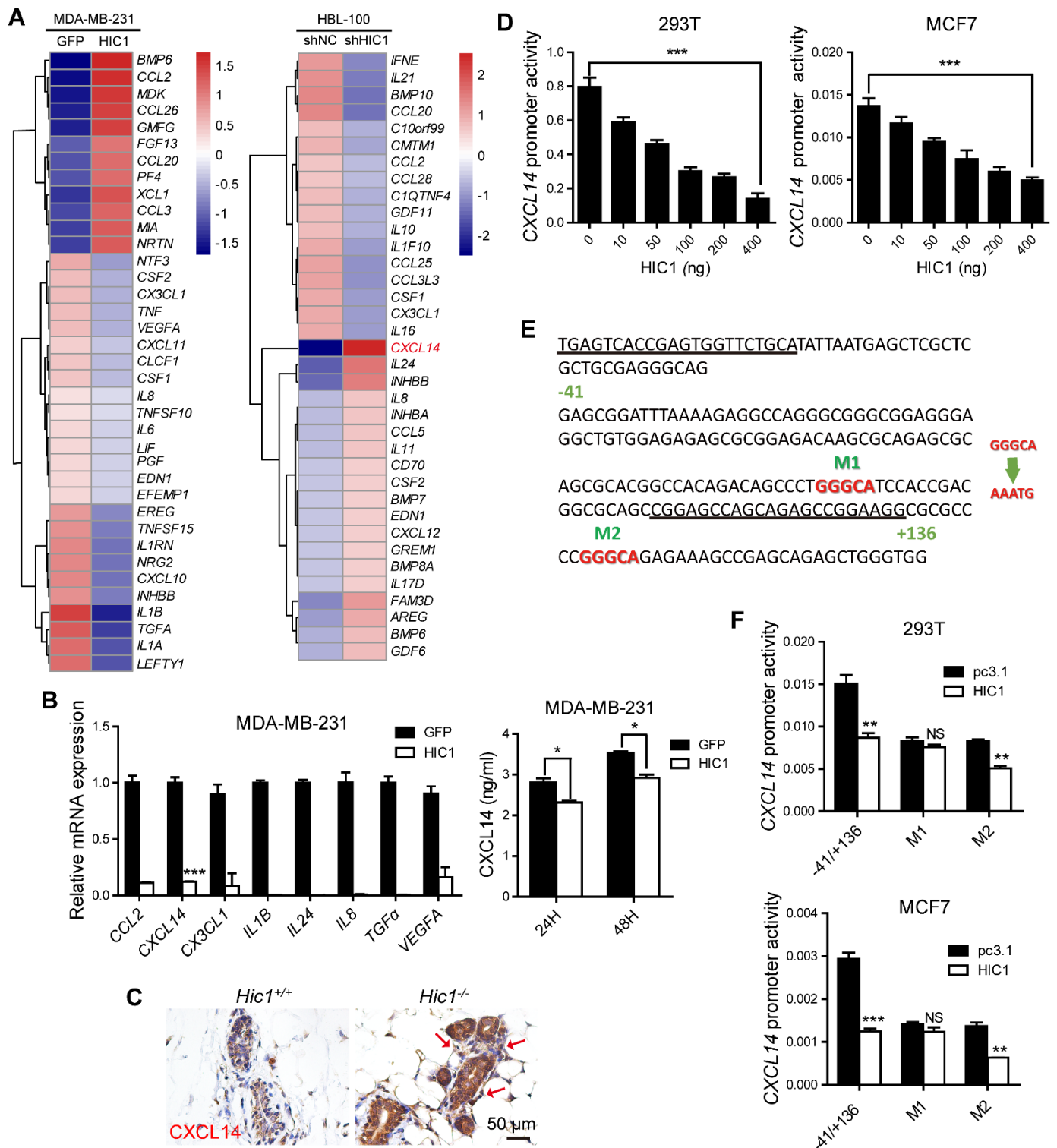


Supplemental figures and figure legends



Supplemental Figure 1. HIC1 deletion induces lactogenic defects of mammary gland in vivo

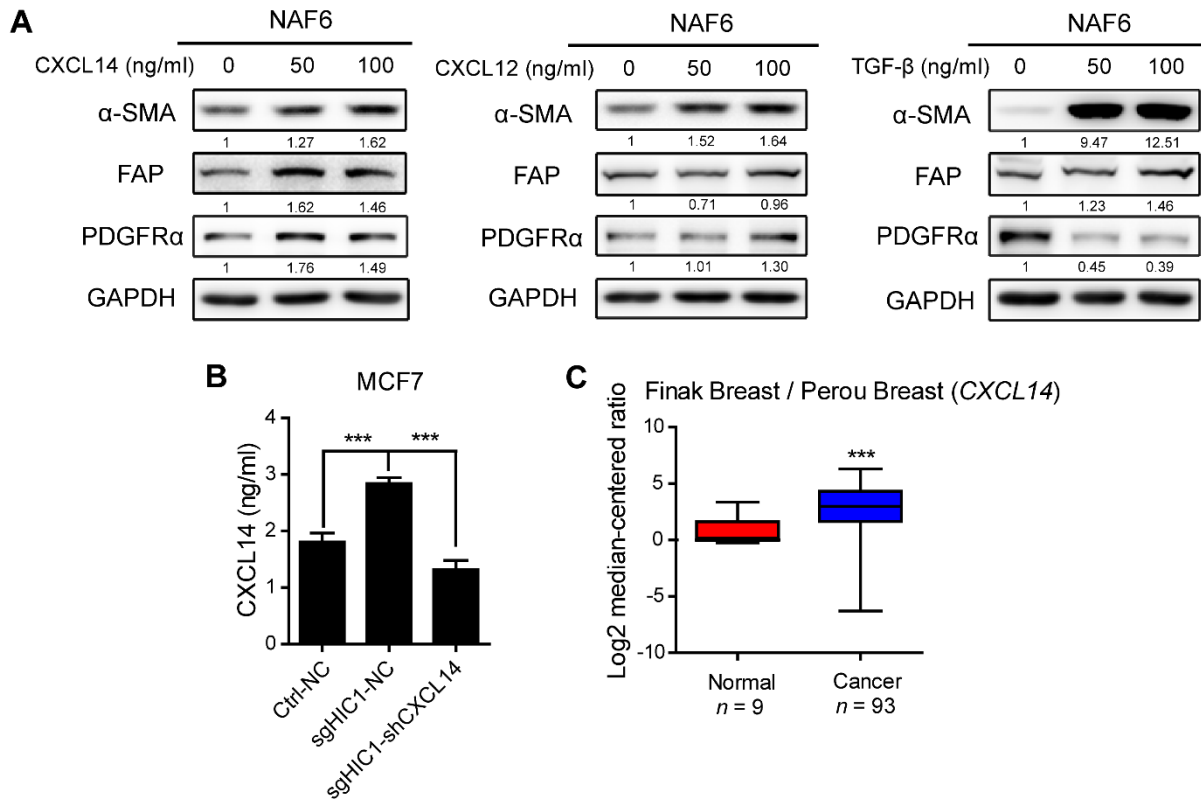
(A) PCR products obtained from mouse tails showing the 1.7-Kb fragment derived from *Wap-Cre* positive mice, the 190-bp fragment from mice carrying the floxed allele, and the 150-bp fragment from mice carrying the wild-type allele. (B) Western blot and RT-qPCR detection of HIC1 expression in mammary, liver, lung and muscle tissues of *Hic1*^{+/+} and *Hic1*^{-/-} mice. The results confirm that HIC1 deletion occurred only in mammary epithelium tissues (mean \pm SEM, $n = 5$ independent experiments; *** $P < 0.001$, P values were obtained using two-tailed Student's t tests). (C) Whole-mount carmine staining of the fourth inguinal mammary glands of mice at 12 months (12 M) or 4 months and day 6 of lactation (L6). (D) Left: percent survival within the first 48 hours after birth of pups nursed by *Hic1*^{+/+} or *Hic1*^{-/-} dams (NS, not significant; P values were obtained using two-tailed Student's t tests). Right: weight gain of pups nursed by *Hic1*^{-/-} or *Hic1*^{+/+} dams. The pups were weighed every 3 days for 13 days (mean \pm SD; *** $P < 0.001$, P values were obtained using repeated measures ANOVA followed by a post-hoc LSD test). (E) H&E staining of the mammary glands of L6 mice. The red arrows indicate lipid droplets. (F) Oil Red-O staining of the mammary glands of L6 mice. The broken lines indicate the alveolar edges. (G) Vasculogenic mimicry (VM) assays of MCF7 cells (Ctrl, sgHIC1-3 and sgHIC1-4). Representative images of vasculogenic networks in the extracellular matrix are shown. (H) Left: Western blot assays of MDA-MB-231 cells with overexpression of HIC1. Right: VM assays of MDA-MB-231 cells. (I) Box plot of *HIC1* mRNA levels at different BrCa grades determined from an Oncomine dataset (Zhao Breast) (NS, not significant; * $P < 0.05$; P values were calculated via one-way ANOVA followed by Bonferroni's post-hoc test).



Supplemental Figure 2. *CXCL14* is modulated by HIC1

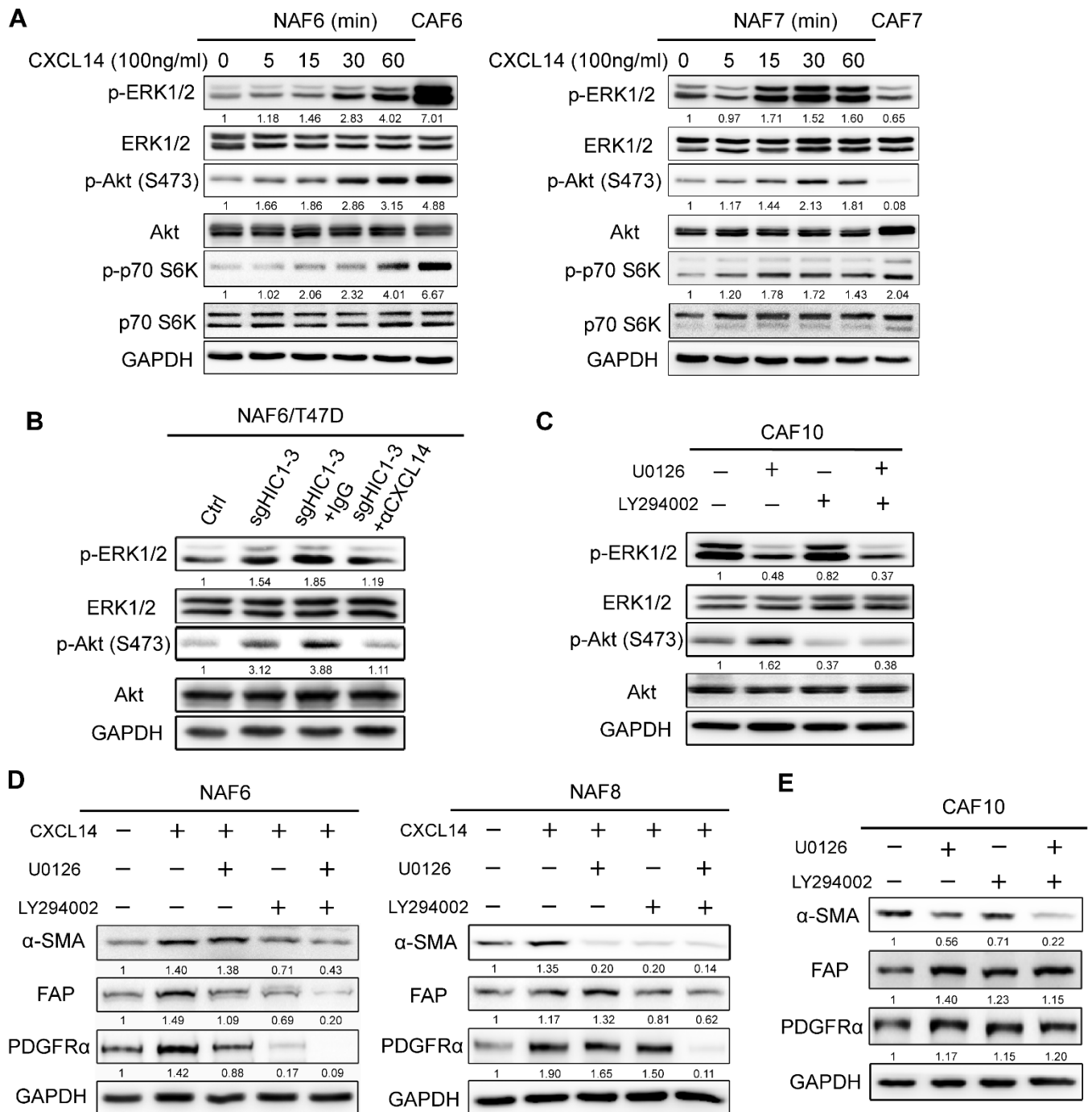
(A) Heat maps of differentially expressed genes encoding cytokines. Rows, genes; columns, experimental cells. (B) Left: relative RT-qPCR analysis of the 8 differentially expressed genes (*CCL2*, *CXCL14*, *CX3CL1*, *IL1B*, *IL24*, *IL8*, *TGFA* and *VEGFA*) observed during overexpression of HIC1 in MDA-MB-231 cells (MDA-MB-231^{HIC1}/MDA-MB-231^{GFP}). Right: ELISA analysis of CXCL14 levels in culture supernatants of MDA-MB-231^{HIC1}/MDA-MB-231^{GFP} cells. The culture supernatants were collected after culture of the cells for 24 h or 48 h. (C) Representative immunohistochemistry for CXCL14 in the mammary gland of 6 M mice. Positive staining in the mammary gland stroma of *Hic1*^{-/-} mice is indicated by red arrows ($n = 3$ for each

group). **(D)** Reporter activity after transient co-transfection of 293T and MCF7 cells with the *CXCL14* full-length (-2000/+136) promoter and increasing amounts of the HIC1 expression vector. The repressive effect increased gradually with the dose of HIC1 expression vector. **(E)** Nucleotide sequence of the -41/+136 construct. Two potential HIC1 binding sites, M1 and M2, were identified and mutated (GGGCA → AAATG). The primers used to amplify the *CXCL14* promoter fragment in the ChIP assay are indicated by black lines. **(F)** Reporter activity of the -41/+136 *CXCL14* promoter and two mutants (M1 and M2) in 293T and MCF7 cells co-transfected with pcDNA3.1 control plasmid or the HIC1 expression plasmid. The results show that the M1 mutated construct markedly neutralized the repressive effect of HIC1 compared with the control (mean ± SEM, $n = 5$ independent experiments; * $P < 0.05$, ** $P < 0.01$, *** $P < 0.001$; P values in B and F were obtained using two-tailed Student's t tests, P values in D were obtained using one-way ANOVA followed by Bonferroni's post-hoc test).



Supplemental Figure 3. CXCL14 treatment has an activating effect similar to that of CXCL12

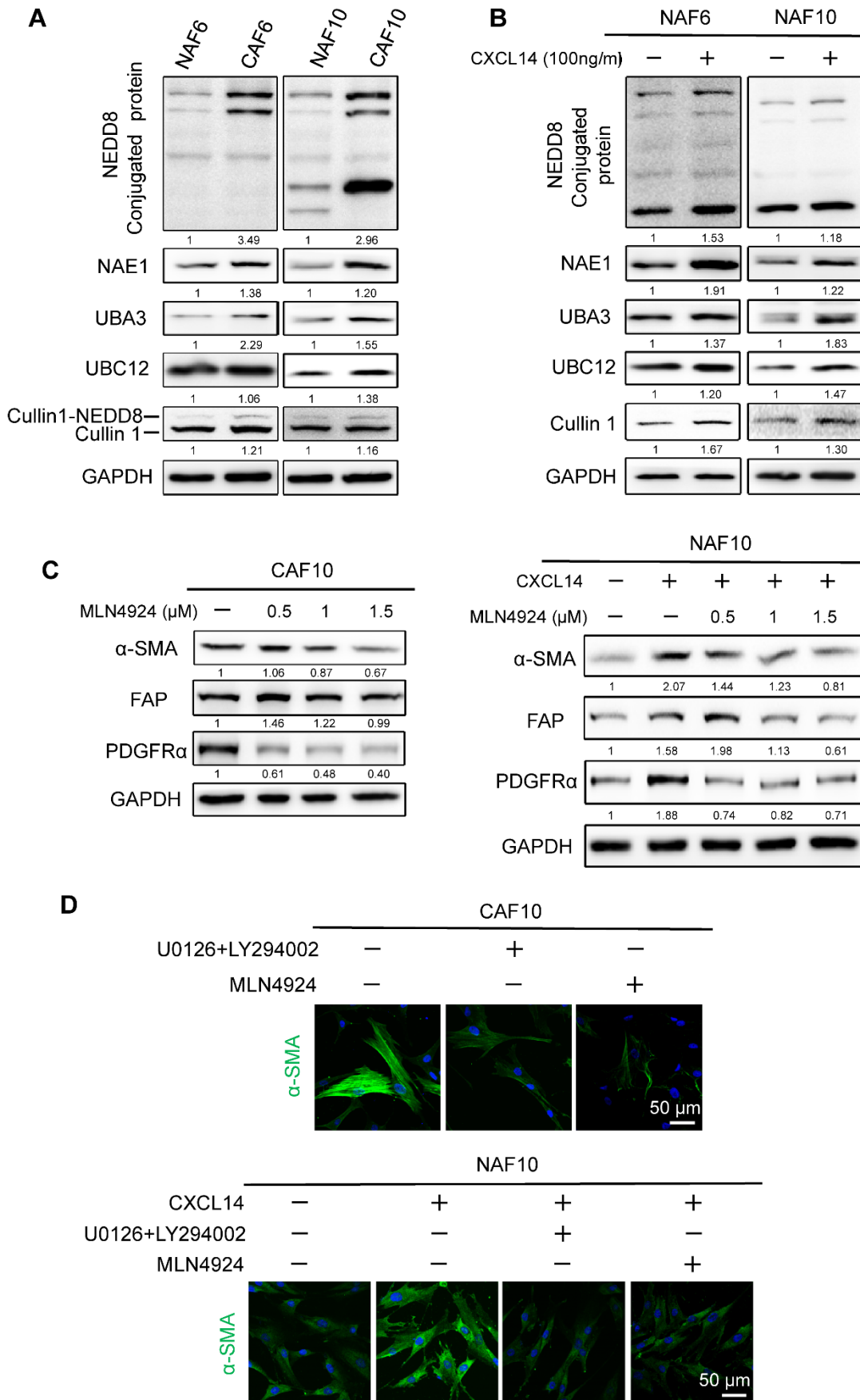
(A) NAF6 cells were treated with rhCXCL14, rhCXCL12 or rhTGF- β at various concentrations (0-100 ng/ml) for 4 days. Lysates of the cells were analyzed by Western blotting with antibodies against α -SMA, FAP, PDGFR α and GAPDH. (B) ELISA analysis of CXCL14 secretion by MCF7^{Ctrl-NC}, MCF7^{sgHIC1-NC} and MCF7^{sgHIC1-shCXCL14} cells that were injected into the mammary fat pads of female BALB/c nude mice (mean \pm SEM, $n = 4$ independent experiments; *** $P < 0.001$, P values were obtained using one-way ANOVA followed by Bonferroni's post-hoc test). (C) Box plot of *CXCL14* mRNA levels determined from two OncoPrint datasets (Finak Breast and Perou Breast) (***) $P < 0.001$, P values were calculated via two-tailed Student's t tests).



Supplemental Figure 4. CXCL14 activates mammary fibroblasts via activation of the ERK1/2 and Akt pathways

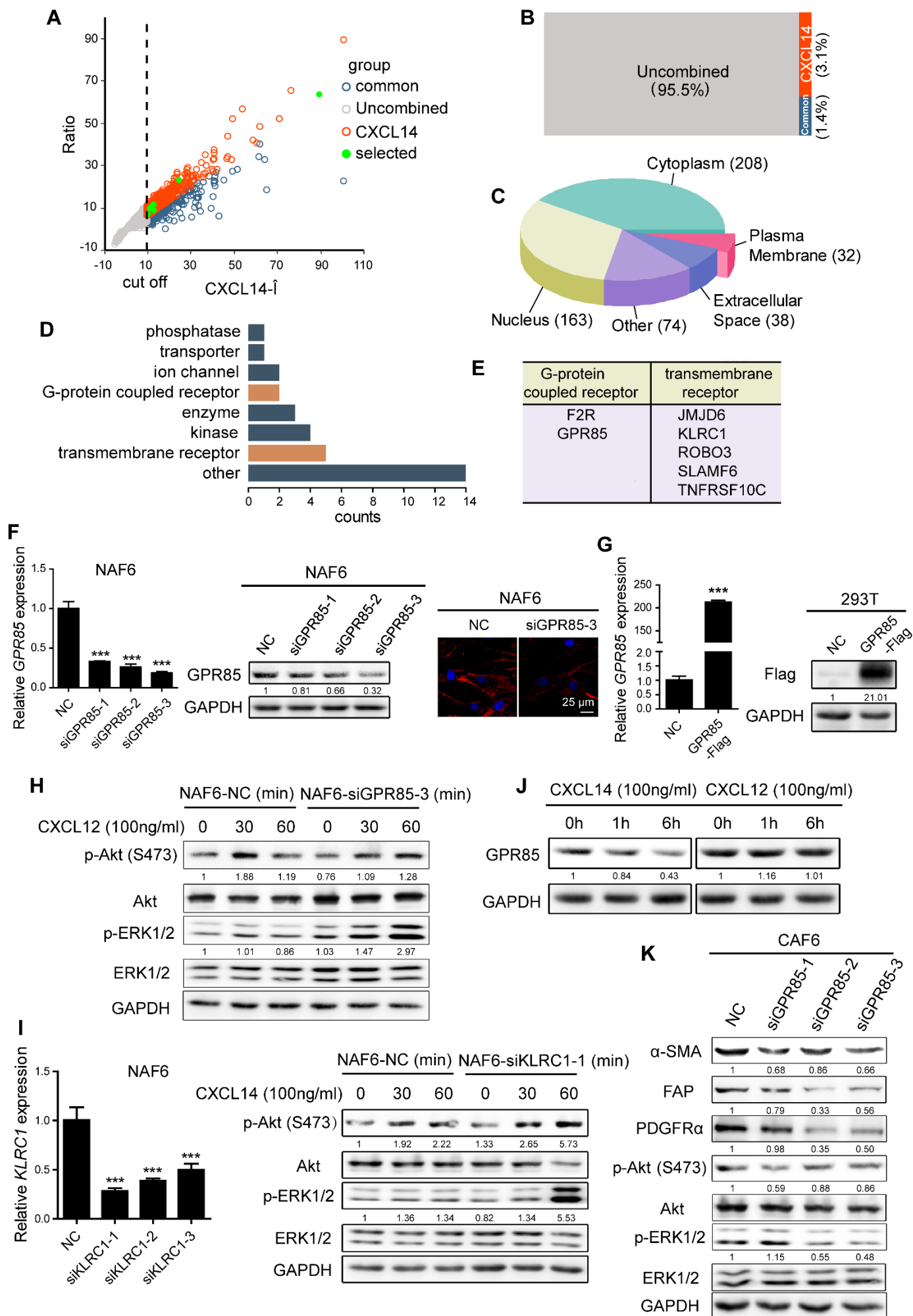
(A) NAF6 and NAF7 cells were treated with rhCXCL14 at 100 ng/ml for the indicated times (0, 5, 15, 30 and 60 minutes); primary CAF6 or CAF7 cells served as the positive controls. Cell lysates were analyzed by Western blotting with antibodies against p-ERK1/2, ERK1/2, p-Akt (Ser 473), Akt, p-p70 S6K, p70 S6K and GAPDH. (B) NAF6 cells were co-cultured with T47D^{Ctrl}/T47D^{sgHIC1} luminal BrCa cells for 4 days in the presence or absence of an antibody against CXCL14 dy (α -CXCL14, 2 μ g/ml) or an isotype-matched IgG control (IgG). Cell lysates were analyzed by Western blotting with antibodies against p-ERK1/2, ERK1/2, p-Akt (Ser 473), Akt and GAPDH. (C) Primary CAF10 cells were treated with U0126 (MEK1/2 inhibitor, 5 μ M), LY294002 (PI3K inhibitor, 5 μ M) or both U0126 and LY294002 for 30 minutes to assay the respective

signal pathways. Lysates of the cells were analyzed by Western blotting with antibodies against p-ERK1/2, ERK1/2, p-Akt (Ser 473), Akt and GAPDH. **(D)** NAF6 and NAF8 cells were treated with BSA or rhCXCL14 at 100 ng/ml in the presence or absence of U0126 (5 μ M), LY294002 (5 μ M) or both inhibitors for 4 days. Lysates of the cells were analyzed by Western blotting with antibodies against α -SMA, FAP, PDGFR α and GAPDH. **(E)** Primary CAF10 cells were treated with U0126 (5 μ M), LY294002 (5 μ M) or both inhibitors for 4 days. Lysates of the cells were analyzed by Western blotting with antibodies against α -SMA, FAP, PDGFR α and GAPDH.



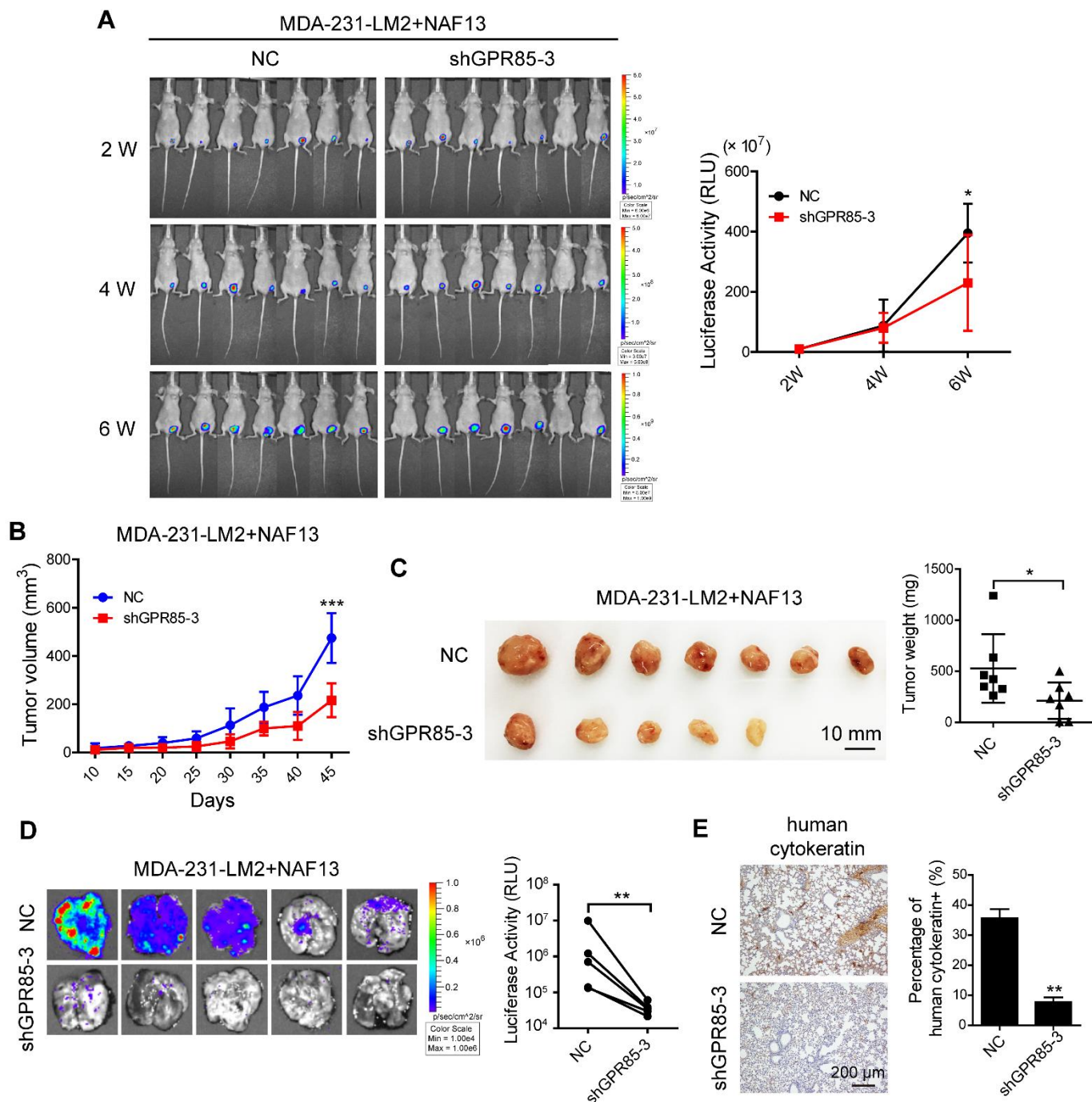
Supplemental Figure 5. CXCL14 activates mammary fibroblasts via overactivation of the neddylation pathway

(A and B) Overactivation of the neddylation pathway in primary CAF6/CAF10 and CXCL14-activated NAF6/NAF10 cells compared with untreated NAF6/NAF10 cells. Immunoblotting was performed to determine the expression of global NEDD8-conjugated proteins, NEDD8-activating enzyme (E1, NAE1 and UBA3 heterodimer), NEDD8-conjugating enzyme (E2, UBC12) and cullin1 (a neddylation substrate) with GAPDH as a loading control. **(C)** Primary CAF10 (left panel) and CXCL14-activated NAF10 (right panel) cells were treated with the NEDD8-activating enzyme inhibitor MLN4924 at the indicated doses (0.5 μ M, 1 μ M and 1.5 μ M) for 4 days. Lysates of the cells were analyzed by Western blotting with antibodies against α -SMA, FAP, PDGFR α and GAPDH. **(D)** Immunofluorescence staining for detection of α -SMA expression by primary CAF10 (upper) and CXCL14-activated NAF10 (lower) cells treated with U0126 (5 μ M) + LY294002 (5 μ M) or MLN492 (1 μ M) for 4 days.



Supplemental Figure 6. GPR85 is a novel functional receptor for CXCL14

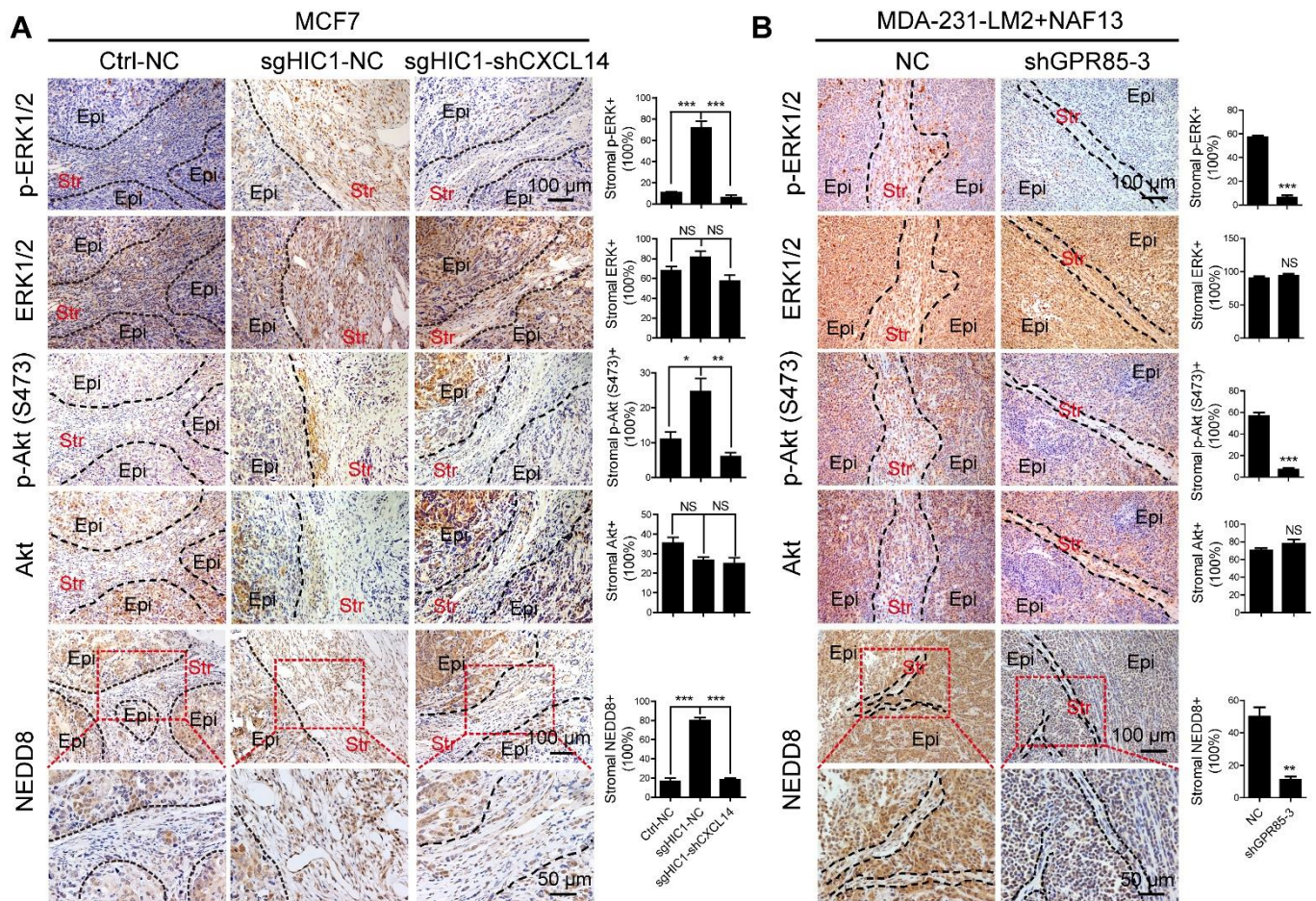
(A) Plots showing the normalized fluorescence intensities (CXCL14- \hat{I} , x-axis) and ratios (CXCL14- \hat{I} /biotin- \hat{I} , y-axis) of all proteins in the human proteome microarrays in the CXCL14 group. The vertical dashed line indicates the threshold (labeled “cut off”). Each circle represents a single protein (brown, CXCL14-uncombined proteins; dark blue, biotin/CXCL14 common combined proteins; red, CXCL14-specific combined proteins; green, selected proteins). **(B)** Of the proteins on the human proteome microarrays, 95.5 percent are CXCL14-uncombined proteins, 1.4 percent are biotin/CXCL14 common combined proteins, and 3.1 percent are CXCL14-specific combined proteins. **(C)** There are 32 plasma membrane proteins among 515 CXCL14-specific combined proteins. **(D)** Classification and corresponding numbers of the 32 plasma membrane proteins. **(E)** Table of selected proteins, including 2 known G protein-coupled receptors and 5 transmembrane receptors. **(F)** Knockdown of GPR85 expression by siRNAs in NAF6 cells. The mRNA and protein levels of GPR85 were confirmed by RT-qPCR, Western blot and immunofluorescence analyses (mean \pm SEM, $n = 5$ independent experiments; $***P < 0.001$, P values were obtained using one-way ANOVA followed by Bonferroni’s post-hoc test). **(G)** Overexpression of GPR85 was confirmed by real-time PCR and Western blotting in 293T cells. **(H)** Knockdown of GPR85 expression by GPR85-3 siRNA in NAF6 cells in the presence and absence of rhCXCL12 at 100 ng/ml for the indicated times (0, 30 and 60 minutes). Cell lysates were analyzed by Western blotting with antibodies against p-Akt (Ser 473), Akt, p-ERK1/2, ERK1/2 and GAPDH. **(I)** Left: knockdown of KLRC1 expression by siRNAs in NAF6 cells. The mRNA levels of KLRC1 were confirmed by RT-qPCR analysis. Right: knockdown of KLRC1 expression by KLRC1-1 siRNA in NAF6 cells in the presence or absence of rhCXCL14 at 100 ng/ml for the indicated times (0, 30 and 60 minutes). Cell lysates were analyzed by Western blotting with antibodies against p-Akt (Ser 473), Akt, p-ERK1/2, ERK1/2 and GAPDH (mean \pm SEM, $n = 5$ independent experiments; $**P < 0.01$, $***P < 0.001$; P values were obtained using one-way ANOVA followed by Bonferroni’s post-hoc test). **(J)** NAF6 cells were treated with rhCXCL14 or rhCXCL12 at 100 ng/ml for the indicated times (0, 1 and 6 hours). Cell lysates were analyzed by Western blotting with antibodies against GPR85 and GAPDH. **(K)** Knockdown of GPR85 expression by siRNAs in CAF6 cells. Cell lysates were analyzed by Western blotting with antibodies against α -SMA, FAP, PDGFR α p-Akt (Ser 473), Akt, p-ERK1/2, ERK1/2 and GAPDH.



Supplemental Figure 7. Knockdown of GPR85 expression in NAFs suppresses lung metastasis of TNBC xenografts

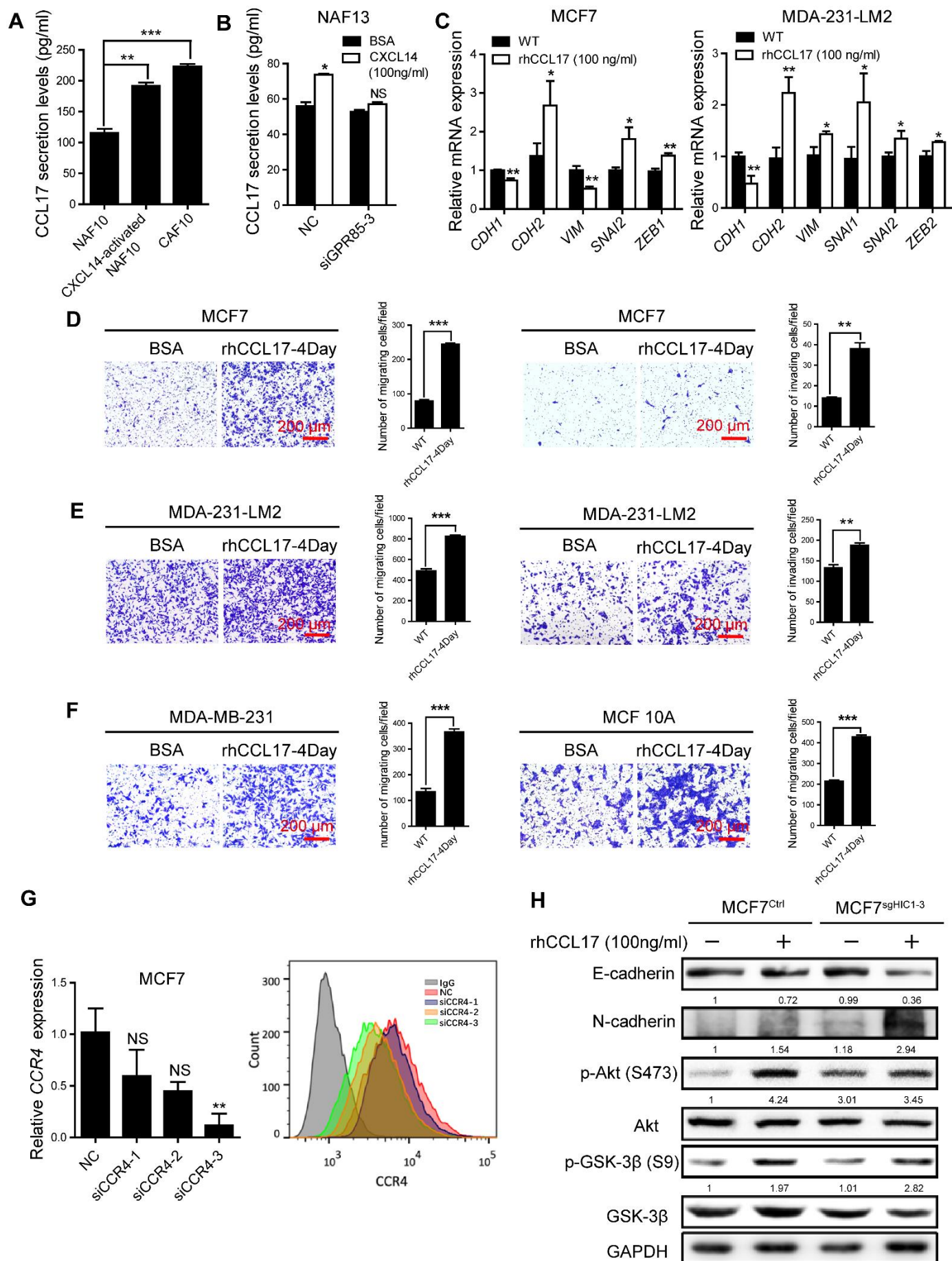
(A) MDA-231-LM2 TNBC cells mixed with NAF13-NC or NAF13-shGPR85-3 cells at a ratio of 3:1 were injected unilaterally into the fourth mammary fat pads of female BALB/c nude mice ($n = 7$ per group). Left: representative bioluminescence images of these mice at the 2nd week (2W), the 4th week (4W) and the 6th week (6W). Right: quantitative analysis of the luciferase activity at 2W, 4W and 6W ($*P < 0.05$, P values were calculated via the Mann-Whitney U test). (B) Tumor volumes were measured with calipers at the indicated time points (mean \pm SD; $***P < 0.001$, P values were obtained using repeated measures ANOVA followed by a post-hoc LSD test). (C) Photographs and weights of the tumors obtained from the animals described in (A) (mean \pm SD; $*P < 0.05$, P values were obtained using two-tailed Student's t tests). (D) Representative

bioluminescence imaging of the harvested lungs (left) and quantification of their bioluminescent signals (right) (mean \pm SD; $**P < 0.01$, P values were obtained using the Mann-Whitney U test). **(E)** Representative immunohistochemical staining for human cytokeratin of each group's lung tissues. The histograms show the mean values for the percentage (%) of human cytokeratin positive cells with statistical evaluation (mean \pm SEM, $n = 3$ independent experiments; $**P < 0.01$, P values were obtained using two-tailed Student's t tests).



Supplemental Figure 8. The activation of stromal ERK1/2, Akt, and neddylation pathways is associated with CXCL14/GPR85 axis in vivo

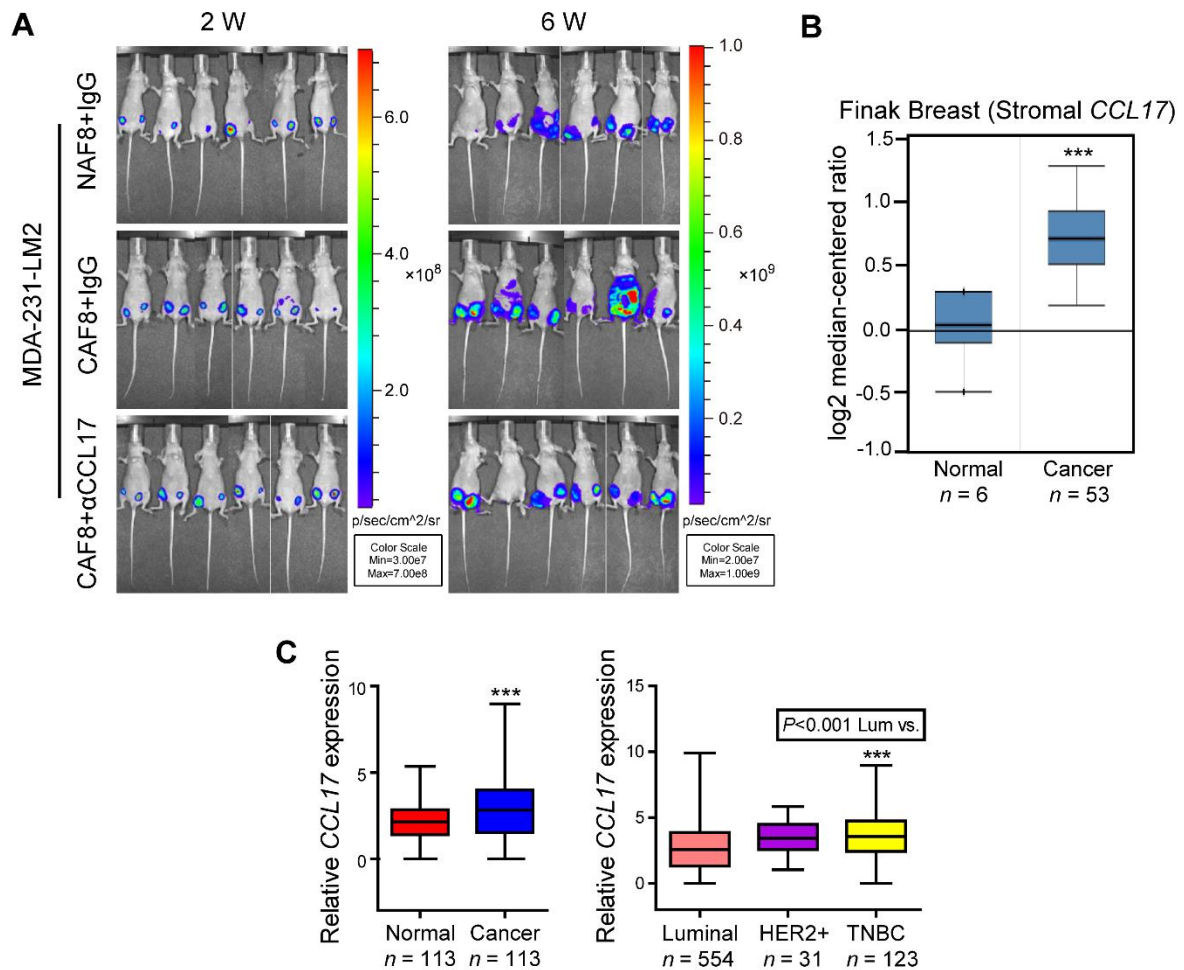
(A) Representative immunohistochemical staining for stromal p-ERK, ERK, p-Akt (S473), Akt and NEDD8 in tumor tissues obtained from each experimental group as described in Figure 4D (Epi, epithelium; Str, stroma). The histograms show the mean value for the percentage (%) of positive cells with the expression of the above-mentioned proteins (mean \pm SEM, $n = 3$ independent experiments; NS, not significant; * $P < 0.05$, ** $P < 0.01$ and *** $P < 0.001$; P values were obtained using one-way ANOVA followed by Bonferroni's post-hoc test). (B) Representative immunohistochemical staining for stromal p-ERK, ERK, p-Akt (S473), Akt and NEDD8 in tumor tissues obtained from each experimental group as described in Supplemental Figure 7A (Epi, epithelium; Str, stroma). The histograms show the mean value for the percentage (%) of positive cells with the expression of the above-mentioned proteins (mean \pm SEM, $n = 3$ independent experiments; NS, not significant; ** $P < 0.01$ and *** $P < 0.001$; P values were obtained using two-tailed Student's t tests).



Supplemental Figure 9. CCL17 induces migration and invasion of BrCa cells

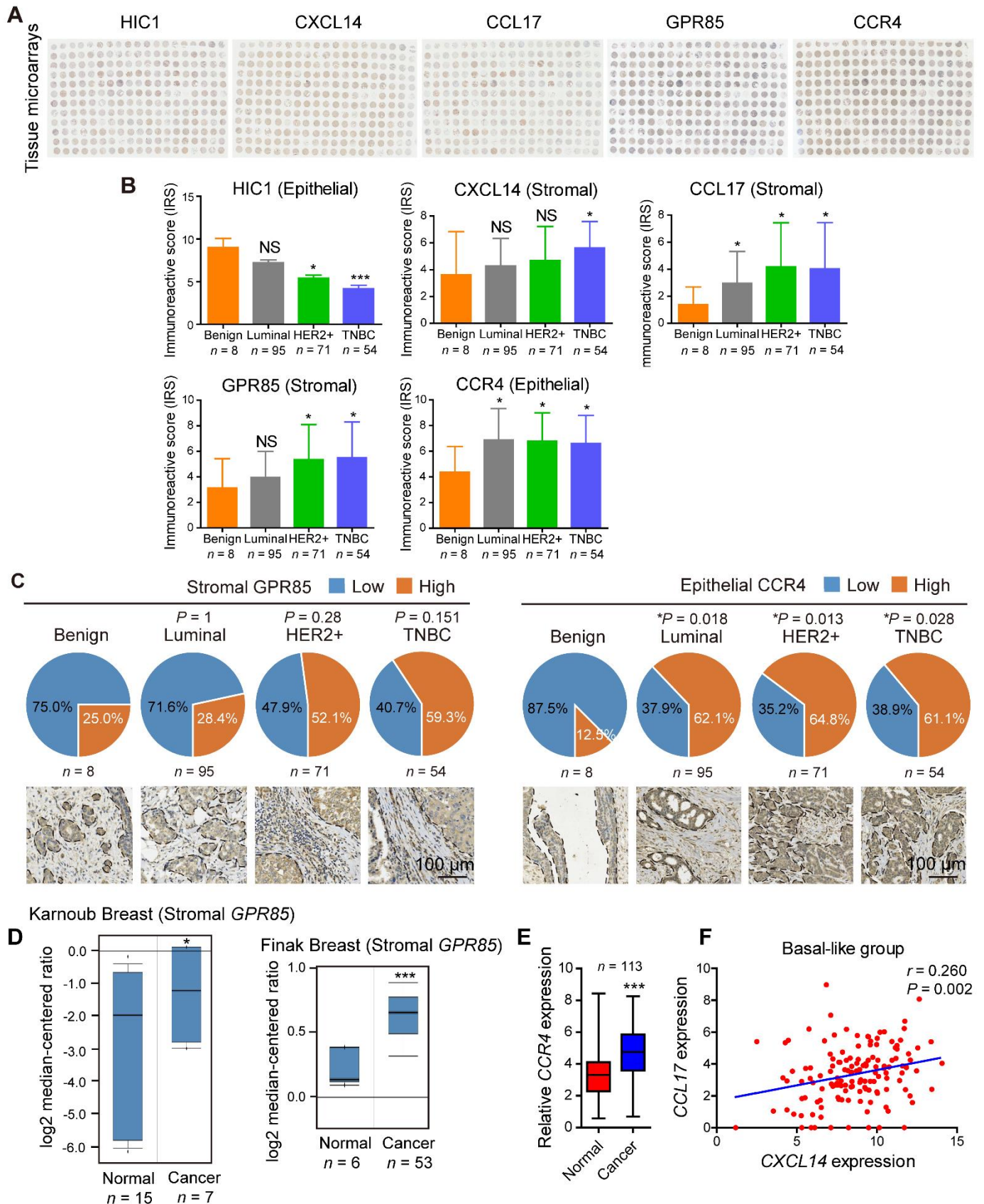
(A) ELISA analyses of CCL17 levels in CM from NAF10, CXCL14-activated NAF10 and CAF10 cells. The culture supernatants were collected after culture of the cells for 48 h. (B) Knockdown of GPR85 expression

by siRNA-3 in NAF13 cells in the presence or absence of rhCXCL14 at 100 ng/ml for 4 days. Then the culture supernatants of these cells were collected and used to analyze CCL17 levels by ELISA assays. **(C)** Relative RT-qPCR analysis of EMT-associated gene expression in MCF7 and MDA-231-LM2 cells after treatment with rhCCL17 (100 ng/ml) for 4 days. **(D and E)** Migration (left) and invasion (right) assays of MCF7 and MDA-231-LM2 cells after treatment with rhCCL17 (100 ng/ml) for 4 days. **(F)** Migration assays of MDA-MB-231 and MCF 10A cells after treatment with rhCCL17 (100 ng/ml) for 4 days. **(G)** Knockdown of CCR4 expression by siRNAs in MCF7 cells. The mRNA and protein levels of CCR4 were confirmed by RT-qPCR and flow cytometry analyses. **(H)** MCF7^{Ctrl} and MCF7^{sgHIC1-3} cells were treated with BSA or rhCCL17 (100 ng/ml) for 4 days. Cell lysates were analyzed by Western blotting with antibodies against E-cadherin, N-cadherin, p-Akt (Ser 473), Akt, p-GSK-3 β (Ser9), GSK-3 β and GAPDH (mean \pm SEM, $n = 5$ independent experiments; NS, not significant; * $P < 0.05$, ** $P < 0.01$, *** $P < 0.001$; P values were obtained using two-tailed Student's t tests in B-F; P values were obtained via one-way ANOVA followed by Bonferroni's post-hoc test in A and G).



Supplemental Figure 10. CCL17 secreted by CAFs promotes lung metastasis of BrCa xenografts

(A) Representative bioluminescence imaging of BALB/c nude mice at the 2nd week (2W) and the 6th week (6W). (B) Box plot of stromal *CCL17* mRNA levels determined from an Oncomine dataset (Finak Breast) (***P* < 0.001, *P* values were calculated via two-tailed Student's *t* tests). (C) Box plot of total *CCL17* expression levels derived from a TCGA dataset (TCGA_BRCA_exp_HiSeqV2-2015-02-24). Left: *CCL17* expression levels in paired normal breast and BrCa tissues (***P* < 0.001, *P* values were calculated via paired *t* tests). Right: *CCL17* expression levels in Luminal (*n* = 554), HER2+ (*n* = 31) and TNBC (*n* = 123) tissues (***P* < 0.001, *P* values were calculated via one-way ANOVA followed by Bonferroni's post-hoc test).



Supplemental Figure 11. The HIC1-CXCL14-CCL17 loop is associated with malignant progression in BrCa patients

(A) The entire field of each TMA chip that was digitally scanned using the Aperio Scanscope XT automated slide scanner. (B) Immunoreactivity scores (IRS) of epithelial HIC1, stromal CXCL14, stromal CCL17, stromal GPR85 and epithelial CCR4 in benign and in various breast cancer subtypes shown as a histogram (P

vs benign: NS, not significant; * $P < 0.05$, ** $P < 0.01$, *** $P < 0.001$; P values were calculated via one-way ANOVA followed by Bonferroni's post-hoc test). **(C)** Upper: the percentages of low and high expression of stromal GPR85 (left) and epithelial CCR4 (right) in benign breast tissue and various breast cancer subtypes are shown as pie charts (P vs benign; P values were obtained using the Chi-square test). Lower: representative IHC images corresponding to the pie charts. The broken lines indicate the margins of the tumor. **(D)** Box plots of stromal *GPR85* mRNA levels determined from two Oncomine datasets (Karnoub Breast and Finak Breast) (* $P < 0.05$ and *** $P < 0.001$, P values were calculated via two-tailed Student's t tests). **(E)** Box plot of *CCR4* expression levels in paired normal breast and BrCa tissues ($n = 113$) derived from a TCGA dataset (TCGA_BRCA_exp_HiSeqV2-2015-02-24) (*** $P < 0.001$, P values were calculated via paired t tests). **(F)** Scatter plots showing the correlation of *CXCL14* expression with *CCL17* expression in Basal-like BrCa patients in the TCGA dataset (TCGA_BRCA_exp_HiSeqV2-2015-02-24). The r value was calculated via Spearman's rank correlation coefficient analysis.

Supplemental methods

Whole-mount staining

Inguinal mammary glands from mice of different age groups as indicated in individual figures were used for whole-mount staining (1). Inguinal fat pads were gently isolated and spread onto a glass slide. Glands were fixed in Carnoy's fixative (ethanol: glacial acetic acid, 75:25) overnight at room temperature. Glands were rehydrated in descending grades of alcohol (70%, 50%, 20%) for 1h each, then washed with distilled water before overnight staining in Carmine alum (1g carmine [Cat. no. C1022; Sigma] and 2.5g aluminium potassium sulfate [Cat. no. A7167; Sigma] were mixed and boiled for 20min in distilled water, filtered and brought to a final volume of 500ml). Stained glands were dehydrated in ascending grades of alcohol (70%, 90%, 100%) for 1h each, and cleared with Methyl salicylate (Cat. no. M2047; Sigma). Samples were examined under a Nikon SMZ1500 dissection microscope.

Oil Red-O staining

ORO staining was performed by staining 8µm mammary cryosections in freshly diluted ORO solution (6 parts 0.5% ORO stock solution [Cat. no. O9755; Sigma] and 4 parts PBS) for 5 min. Sections were rinsed twice with 60% isopropanol, once with water, and then counterstained with Mayer's hematoxylin for 2 min before photography as above.

Primers for PCR-based genotyping of transgene mice

HIC1 forward: 5'-CCCCACCTTTCTACACCTCA-3'

HIC1 reverse: 5'-GAGAGGCAGGGTTCTCCTTT-3'

WAP-Cre forward: 5'-GGCCCGCGCTGGAGTTTCAATAC-3'

WAP-Cre reverse: 5'-GCAACCGCTTCCCCGACTTCCTTA-3'

Immunohistochemistry (IHC) and immunofluorescence (IF) staining

Mammary glands, mouse xenografts and lungs were fixed in 4% formaldehyde overnight at room temperature and embedded in paraffin. Sections of 4 µm in thickness were used for hematoxylin–eosin (H&E) staining, immunofluorescent staining and immunohistochemistry. Samples were baked at 60 °C for 4h, then de-paraffinized by three 10-min extractions in 100% xylene, followed by 5-min each of descending grade of alcohol (100%, 95%, 80% and 70%). Samples were then washed briefly with phosphate-buffered saline (PBS) before transferring to boiling 10 mM sodium citrate buffer (pH 6.0) for 30 min. For immunohistochemistry, sections were pre-treated with 3% hydrogen peroxide for 10 min before blocking. Blocking was performed with 5% normal goat serum in PBS for 30 min at room temperature followed by primary antibody incubation overnight at 4°C. For detection with primary antibody using the immune enzymatic method, the ABC peroxidase detection system (Cat. no. PK-6105; Vector Labs) was used with

3, 3'-diaminobenzidine (DAB) as substrate (Cat. no. SK-4105; Vector Labs) according to manufacturer's instruction. The quantitative results for IHC images were calculated by ImageJ software.

For immunofluorescence stainings, sections and NAFs/CAFs were incubated with Alexa Fluor-488 and Alexa Fluor-594-conjugated secondary antibodies (Jackson Immumoresearch), mounted with 1 μ g/ml DAPI (Vector Labs) to stain nucleus, and examined with a LeicaSP5 confocal microscope.

The primary antibodies are listed the below: K8 (Cat. no. ab59400; Abcam), Ki67 (Cat. no. ab66155; Abcam), cyclin D1 (Cat. no. ab16663; Abcam), α -SMA (Cat. no. ab5694, ab7817; Abcam), FAP (Cat. no. ab28244; Abcam), PDGFR α (Cat. no. ab65258; Abcam), CXCL14 (Cat. no. ab137541; Abcam), p-ERK1/2 (Cat. no. 4370S; CST), ERK1/2 (Cat. no. 9102S; CST), p-Akt (Ser 473) (Cat. no. 4060S; CST), Akt (Cat. no. 4691S; CST), NEDD8 (Cat. no. 2754S; CST), N-cadherin (Cat. no. ab76011; Abcam), vimentin (Cat. no. 5741S; CST), human cytokeratin (Cat. no. ab756; Abcam), GPR85 (Cat. no. ab140783; Abcam) and CCR4 (Cat. no. ab1669; Abcam).

Isolation of primary fibroblasts and culture

We extracted primary fibroblasts from human invasive mammary ductal carcinomas and benign breast mass obtained from mastectomies. All tissues were minced with scalpels and then enzymatically dissociated in DMEM/F12 medium (Cat. no. 11330-032; GIBCO) supplemented with 2% bovine serum albumin, 10ng/mL cholera toxin (Cat. no. c8052; Sigma), 300 units/mL collagenase (Cat. no. 17018-029; Invitrogen), and 100 units/mL hyaluronidase (Cat. no. H3506; Sigma) at 37°C for 18 h. On the second day, the digested suspension was centrifuged at 600 rpm for 4 min to separate the epithelial and fibroblast cells. The supernate was collected for centrifugation at 800 rpm for 10 min to pellet the fibroblasts. The cell pellet was resuspended in DMEM/F12 medium supplemented with 10% fetal bovine serum (GEMINI) and 5 μ g/mL insulin (Cat. no. 40112ES25; YEASEN) and plated in cell culture flasks kept undisturbed for 2 days. All tissues were obtained from the Cooperative Renji Hospital approval or from ductal breast carcinoma patients with approval of the hospital ethical committee and by the patient's written informed consent (Shanghai, China). All fibroblasts were numbered according to the operating time sequence.

Western blots and antibodies

Protein extracts were resolved through 8%-15% SDS-PAGE, transferred to PVDF membranes, and probed with primary antibodies. Peroxidase-conjugated anti-mouse or rabbit antibody (Jackson Immumoresearch) was used as secondary antibody and the antigen-antibody reaction was visualized by enhanced chemiluminescence assay. The quantitative results for Western blots were calculated by ImageJ software.

The commercial antibodies of the following were used: anti-human HIC1 (Cat. no. H8539; Sigma), GAPDH (Cat. no. 30203ES50; YEASEN), α -SMA (Cat. no. ab5694; Abcam), FAP (Cat. no. ab28244; Abcam), PDGFR α (Cat. no. ab134123; Abcam), biotin (Cat. no. 7075; CST), p-ERK1/2 (Cat. no. 4370S; CST), ERK1/2

(Cat. no. 9102S; CST), p-Akt (Ser 473) (Cat. no. 4060S; CST), Akt (Cat. no. 4691S; CST), p-P70 S6K (Cat. no. 9204S; CST), P70 S6K (Cat. no. 9202S; CST), p-GSK-3 β (Cat. no. 9323S; CST), GSK-3 β (Cat. no. 12456S; CST), NEDD8 (Cat. no. 2754S; CST), NAE1 (Cat. no. ab187142; Abcam), UBA3 (Cat. no. ab124728; Abcam), UBC12 (Cat. no. ab109507; Abcam), cullin1 (Cat. no. ab75817; Abcam), GPR85 (Cat. no. ab135332; Abcam), Flag (Cat. No. F3165; sigma), E-cadherin (Cat. no. 3195S; CST), N-cadherin (Cat. no. ab76011; Abcam), vimentin (Cat. no. 5741S; CST) and anti-mouse HIC1 (Cat. no. bs-15485R; Bioss).

Vasculogenic mimicry (VM) formation

MCF7 and MDA-MB-231 cells were allowed to grow to 80% confluence of monolayer. For vasculogenic mimicry assay, matrigel matrix TM (Cat. no. 354248; BD) pre-thawed at 4°C were added into the inner well of μ -slides (Cat. no. 81506; ibidi) and incubated for at least 30 minutes at 37°C until polymerization. 50 μ l of cells (2×10^5 cells/ml) were added onto the polymerized matrix. Microscopy images were taken between 4-24h.

ELISAs

Quantification of CXCL14 and CCL17 levels in the supernate of BrCa cells or fibroblasts were calculated by ELISA assay according to the protocol in the ELISA kit (CXCL14: Cat. no. DY866, CCL17: Cat. no. DY364; R&D Systems). All experiments were done with 4 wells per experiment and repeated three times.

Luciferase reporter assay

Constructs of the *CXCL14* promoter region at -2000/+136, -726/+136, -276/+136 and -41/+136 were generated from genomic DNA of MCF10A cells. *CXCL14* promoter construct pGL3-41/+136 contains two HIC1-responsive elements (HiREs), all of which were mutated (GGGCA \rightarrow AAATG, M1 and M2) by using KOD-Plus Mutagenesis kit followed by the instructions provided by the manufacturer (Cat. no. SMK-101; TOYOBO). MCF7 and 293T cells were maintained in DMEM containing 10% FBS and transfected by Lipofectamine™ 2000 Reagent in 24-well plates. The HIC1 plasmid: *CXCL14* promoter constructs: Renilla plasmid DNA (100ng: 200ng: 20ng) were co-transfected for 6–9 h and then incubated for 24h in fresh complete medium. Cells were then rinsed in cold PBS and lysed with the luciferase assay buffer. Luciferase activities were measured by using a dual luciferase assay kit (Cat. no. E1960; Promega) with a Berthold chemiluminometer (Berthold Detection Systems GmbH, Pforzheim, Germany). The results were expressed as ratio of firefly luciferase activity to Renilla luciferase activity. Data were expressed as the mean values and standard deviations from at least three independent transfections performed in triplicate.

Chromatin immunoprecipitation (ChIP)

In brief, formaldehyde was added directly to the cultured MCF7 or T47D cells in 10 cm plates to a final concentration of 1% for 10 min at room temperature. The cross-linking was stopped by adding glycine to a final concentration of 0.125 M. After 10 min at room temperature, cells were lysed directly in the plates by

resuspension in 1 ml cell lysis buffer for 10 min. Then, the samples were pelleted and resuspended in 1 ml nuclear lysis buffer and sonicated to obtain chromatin fractions from 200bp to 1000bp using a BioRuptor (Diagenode, Liege, Belgium). After preclearing with a 50% slurry of protein A-G beads (Santa Cruz, Delaware Ave, CA, USA) preincubated with salmon sperm DNA and bovine serum albumin for 4-6 h, at 4 °C, the chromatin was incubated with anti-HIC1 antibody (Cat. no. H8539; Sigma) or normal rabbit IgG overnight. The antibody bound chromatin was then pulled down for 3 h with protein A-G beads, washed extensively (low salt wash buffer, high salt wash buffer, LiCl wash buffer, and TE wash buffer) and eluted two times with Elution buffer. After addition of 8 µl of 5M NaCl, the cross-linking was reversed by overnight incubation at 65 °C. The immunoprecipitated DNAs as well as whole cell extract DNAs (input) were preliminarily purified by treatment with RNase A and then proteinase K followed by further purification with an UltraClean™ 15 DNA Purification Kit (Cat. no. U11B10, MoBio experiment diagnosis company) (2). The purified DNA was used for PCR analyses using the relevant primers for *CXCL14* and *GAPDH*. The PCR specific primers for *CXCL14* promoter region at -276/+136 alongside HIC1-responsive elements (HiREs). Only one PCR product for *CXCL14* promoter region was amplified successfully under the following conditions: initial denaturation, 94°C for 1min; denaturation, 94°C for 15s; annealing, 60°C for 30s, extension, 68°C for 20s, altogether 25 cycles; 68°C extension for 5 min (Cat. no. KOD-201; TOYOBO). A control primer specific for the human *GAPDH* promoter region was used for monitoring the experiment.

The primer sequences are as following:

CXCL14 promoter forward: 5'-TGAGTCACCGAGTGGTTCTGCA-3'

CXCL14 promoter reverse: 5'-CCTTCCGGCTCTGCTGGCTCCG-3'

GAPDH promoter forward: 5'-TACTAGCGGTTTTACGGGCG-3'

GAPDH promoter reverse: 5'-TCGAACAGGAGGAGCAGAGAGCGA-3'

Cell migration and invasion assay

BD Falcon cell culture inserts (8 µm) were used for the cell migration assay (Cat. no. 353097, BD), and the inserts precoated with Matrigel (BD) were used for examining cell invasion. Cells were detached from the plates, and the cell suspension was placed into the upper chamber in 0.2 ml of DMEM serum-free medium (1.5×10^4 - 1×10^5 cells per filter). DMEM medium supplemented with 10% FBS was placed in the lower chamber as a chemoattractant. Migration or invasion was scored following 20h. Cells at lower surface of the inserts were then fixed in 4% formaldehyde for 30 min at room temperature, stained using coomassie brilliant blue for 30 min, visualized and counted. Values for cell migration or invasion were expressed as the mean number of cells per microscopic field over five fields per one insert for triplicate experiments. Experiments were repeated at least three times.

siRNAs transfection

The BrCa cells and NAFs were transfected with Lipofectamine® 3000 (Invitrogen) in serum-free Opti-MEM (Gibco) according to the instruction manual. All siRNAs were synthesized from Biotend (Shanghai, China). The sense and anti-sense strands of siRNAs were as follows:

CCR4 siRNA-1 sense: 5'-CACCUUACAACAUAAGUGCUdTdT-3'

CCR4 siRNA-1 antisense: 5'-AGCACUAUGUUGUAAGGUGdTdT-3'

CCR4 siRNA-2 sense: 5'-GCAAGUACAUCCUACAGCUdTdT-3'

CCR4 siRNA-2 antisense: 5'-AGCUGUAGGAUGUACUUGCdTdT-3'

CCR4 siRNA-3 sense: 5'-GUUAUACUGAGCGCAACCAdTdT-3'

CCR4 siRNA-3 antisense: 5'-UGGUUGCGCUCAGUAUAACdTdT-3'

GPR85 siRNA-1 sense: 5'-GCAUCAGUGUCACCAGAUAdTdT-3'

GPR85 siRNA-1 antisense: 5'-UAUCUGGUGACACUGAUGCdTdT-3'

GPR85 siRNA-2 sense: 5'-GGUCUUAGACGAGUUCAAAdTdT-3'

GPR85 siRNA-2 antisense: 5'-UUUGAACUCGUCUAAGACCDdTdT-3'

GPR85 siRNA-3 sense: 5'-GGCACUUACUCAUUCAUAdTdT-3'

GPR85 siRNA-3 antisense: 5'-UAAUGAAUGAGUAAGUGCCdTdT-3'

KLRC1 siRNA-1 sense: 5'-GUUAUUCCCUCUACAUAAdTdT-3'

KLRC1 siRNA-1 antisense: 5'-UUAAUGUAGAGGGAAUAAdTdT-3'

KLRC1 siRNA-2 sense: 5'-CUAUCACUGCAAAGAUUUAdTdT-3'

KLRC1 siRNA-2 antisense: 5'-UAAAUCUUUGCAGUGAUAGdTdT-3'

KLRC1 siRNA-3 sense: 5'-CUAUCACUGCAAAGAUUUAdTdT-3'

KLRC1 siRNA-3 antisense: 5'-UAAAUCUUUGCAGUGAUAGdTdT-3'

RT-qPCR

Reverse transcription–quantitative real-time PCR (RT-qPCR) was performed with an Applied Biosystems 7500 Fast Real-Time PCR System (ABI, Foster, USA), using the Hidff qPCR SYBR Green Master Mix (Cat. no. 11202ES08; YEASEN) according to the manufacturer's instruction. All reactions were done in a 20ul reaction volume in triplicate. Primers were obtained from GENEWIZ. Following an initial denaturation at 95 °C for 30s, 40 cycles of PCR amplification were performed at 95 °C for 5s and 60 °C for 30s. Standard curves were generated and the relative amount of target gene mRNA was normalized to GAPDH.

The primer sequences are as following:

Mouse

HIC1 forward: 5'-GTCTCTGCTTCCGAGGTGTC-3'

HIC1 reverse: 5'-CAGCTAAAGTTGGGCTCAGG-3'

CXCL14 forward: 5'-CGTGGACGGGTCCAAGTGTA-3'

CXCL14 reverse: 5'-CCGGTACCTGGACATGCTCTT-3'

SIRT1 forward: 5'-CGGAGGGCCAGAGAGGCAGT-3'

SIRT1 reverse: 5'-CTCTTGCGGAGCGGCTCGTC-3'

GAPDH forward: 5'-TGTGTCCGTCGTGGATCTGA-3'

GAPDH reverse: 5'-TTGCTGTTGAAGTCGCAGGAG-3'

Human

HIC1 forward: 5'-GTCGTGCGACAAGAGCTACAA-3'

HIC1 reverse: 5'-CGTTGCTGTGCGAACTTGC-3'

GAPDH forward: 5'-ACGGATTTGGTCGTATTGGG-3'

GAPDH reverse: 5'-CGCTCCTGGAAGATGGTGAT-3'

CCL2 forward: 5'-CAGCCAGATGCAATCAATGCC-3'

CCL2 reverse: 5'-TGGAATCCTGAACCCACTTCT-3'

CCL20 forward: 5'- CCGTATTCTTCATCCTAA -3'

CCL20 reverse: 5'-TTCACCCAAGTCTGTTT-3'

CXCL14 forward: 5'-GCACCAAGCGCTTCATCAA-3'

CXCL14 reverse: 5'-TCGTAGACCCTGCGCTTCTC-3'

CX3CL1 forward: 5'-CGCGTTCTTCCATTTGTGTA-3'

CX3CL1 reverse: 5'-CTGTGTCGTCTCCAGGACAA-3'

IL1B forward: 5'-ATGGCTTATTACAGTGGC-3'

IL1B reverse: 5'-GTAGTGGTGGTCGGAGA-3'

IL24 forward: 5'-ATGGTTGTGCTCCCTTGC-3'

IL24 reverse: 5'-CGGGCACTCGTGATGTTAT-3'

IL8 forward: 5'-TAAAGACATACTCCAAACC-3'

IL8 reverse: 5'-ACTTCTCCACAACCCTC-3'

TGF α forward: 5'-GCCCTGGCTGTCCTTAT-3'

TGF α reverse: 5'-AGCGGTTCTTCCCTTCA-3'

VEGFA forward: 5'-CGGCGTCGCACTGAAA-3'

VEGFA reverse: 5'-CGGCTGGAGCACTGTCT-3'

CCL20 forward: 5'-CCGTATTCTTCATCCTAA-3'

CCL20 reverse: 5'-TTCACCCAAGTCTGTTT-3'

E-cadherin forward: 5'-CTGCCAGAAAATGAAAAAGG-3'

E-cadherin reverse: 5'-AGTGTATGTGGCAATGCGTTC-3'

N-cadherin forward: 5'-ATCTCGGGTCAGCTGTCCG-3'

N-cadherin reverse: 5'-GGCTATCTGCTCGCGATCC-3'

vimentin forward: 5'-ATGACCGCTTCGCCAACTAC-3'

vimentin reverse: 5'-GACTTGCCTTGGCCCTTGA-3'

Slug forward: 5'-TGTGTGGACTACCGCTGCTC-3'

Slug reverse: 5'-GAGAGGCCATTGGGTAGCTG-3'

Zeb1 forward: 5'-AAGTGGCGGTAGATGGTA-3'

Zeb1 reverse: 5'-TGTTGTATGGGTGAAGCA-3'

Zeb2 forward: 5'-TTCTGCGACATAAATACG-3'

Zeb2 reverse: 5'-GAGTGAAGCCTTGAGTGC-3'

Construction of lentiviral vectors

The Cas9 expression constructs Lenticas9-blast and the sgRNA expression plasmid Lentiguid-puro was used to generate stable HIC1 knockout MCF7 and T47D cell line. The insert sgRNA sequences to silence HIC1 are as following:

name	Target sequence:
SgHIC1-1	CGCACGGAATGCACACGTACAGG
SgHIC1-2	TCTTGTCGCACGACGCGCAGCGG
SgHIC1-3	TGCGCCGAGCTGTACGCGTCGGG
SgHIC1-4	CCGCCGCGAAATGGGTCGGAAGG

For generation of a stable CXCL14 knockdown MCF7 cell line, GV113 lentiviral vectors expressing short hairpin RNAs targeting CXCL14 were purchased from GeneChem Company (Shanghai, China). Lentiviruses were produced and infected cells were selected by RFP. Four shRNAs (clone ID: CXCL14-RNAi-37874, 37875, 37876 and 37877) were used in the experiment, namely shCXCL14-1, 2, 3 and 4.

ID	Target sequence:	Site	GC (%)
ShCXCL14-1	GCAGGGTCTACGAAGAATA	780	47.37
ShCXCL14-2	GCTTCATCAAGTGGTACAA	744	42.11
ShCXCL14-3	AGGAGAAGATGGTTATCAT	654	36.84
ShCXCL14-4	ACGTGAAGAAGCTGGAAAT	612	42.11

For generation of a stable GPR85 knockdown NAF13 cells, GV248 lentiviral vectors expressing short hairpin RNAs targeting GPR85 were purchased from GeneChem Company (Shanghai, China). Lentiviruses were produced and infected cells were selected by GFP. One shRNA with the same sequence as siGPR85-3 (clone ID: GPR85-RNAi-65669-1) was used in the experiment, namely shGPR85-3.

ID	Target sequence:	GC (%)
ShCXCL14-3	GGCACTTACTCATTGATTA	36.84

For generation of stable HIC1 overexpression in MDA-MB-231 cells, human full length HIC1 cDNA was inserted into the lentivirus vector PHR-SIN-CSIGW.

Human proteome microarrays

We utilized a human proteome microarray (Wayen Biotechnologies (Shanghai), Inc.) that constructed from a library of 18,583 unique full-length human ORFs, as described previously (3). Proteome microarrays were blocked with blocking buffer (5% BSA in 0.1% Tween 20; PBST) for 1.5 h at room temperature with gentle agitation; CXCL14-biotin or biotin was diluted to 5 µg/ml in PBST and incubated on the blocked proteome microarray at room temperature for 1 h. The microarrays were washed with PBST three times for 5 min each washing and were incubated with Cy5-Streptavidin for 1 h at room temperature, followed by three 5 min washes in PBST. The microarrays were spun dry at 250 × g for 3 min and were scanned with a GenePix 4000B microarray scanner (Axon Instruments, USA) to visualize and record the results. GenePix™ Pro v6.0 software was used for data analysis.

Validating CXCL14–protein interaction by streptavidin agarose affinity assay

Primary NAF cells were lysed with IP lysis buffer and incubated with 6 µg BSA or CXCL14-bioin overnight at 4°C. The samples were then incubated with 60 µL of NeutrAvidin Agarose Resin (Cat. no. 29201; Thermo Scientific) at 4°C for 4 h. Centrifuge for 1-2 minutes at ~2500 × g and remove the supernatant. The resin-bound complex was then washed with IP lysis buffer three times, followed by boiling in SDS-PAGE sample buffer.

Calcium mobilization assay

NAF6 cells were plated on glass-bottom dishes 24 h prior to the experiment. Cells were washed with Hank's balanced salt solution (HBSS) containing 1 mg/mL of bovine serum albumin (BSA) and loaded with 5 µM Fluo 4-AM (Cat. no. F312; Dojindo) by incubation for 30 min in cell culture incubator. After washing twice with HBSS-BSA, cells were incubated in HBSS-BSA in cell culture incubator for 20 min. Then the dynamic fluorescence changes of the cells after different stimulation were examined with a LeicaSP5 confocal microscope.

Generation of GPR85-expressing vector

The plasmid expressing GPR85 was obtained from OriGene (TrueORF Gold cDNA Clones, Cat. no. RC205181). This plasmid was pCMV6-ENTRY, which carried the tag of Myc and Flag.

Binding assays

Competition experiments were completed by Jiangsu Institute of Nuclear Medicine and performed using 10 nM ^{125}I -labeled CXCL14 and indicated concentrations of unlabeled chemokines as previously described (4). Briefly, ^{125}I -labeled CXCL14 was incubated with 1×10^6 cells resuspended in binding buffer (50nM HEPES, pH 7.2, 1 mM CaCl_2 , 5mM MgCl_2 , 0.5% BSA) in the presence or absence of unlabeled chemokines. After incubation at room temperature for 30 min, the cells were pelleted through a PBS cushion with 10% sucrose for 1 min at $10,000 \times g$. The supernatant was removed and the radioactivity associated with cell pellets was measured using a γ -counter (CliniGamma, Pharmacia). Each data point was determined in triplicate. Binding data were analyzed with Prism computer program by GraphPad (San Diego, CA), with IC50 representing the concentration of radioligand required to reach half-maximal binding.

Co-culture

To assay the effect of BrCa cells on fibroblasts, MCF7/T47D cells (3×10^5) were added into the upper chamber and fibroblasts (5×10^4) were added into the lower chamber of a 6-well cell culture insert with 0.4 μm pore size (Merk Millipore). Selected co-cultures were treated neutralizing antibodies to CXCL14 (Cat. no. MAB866, R&D Systems) at 1 $\mu\text{g}/\text{ml}$ for 4 days followed by Western blot and immunofluorescence assays.

To assay the effect of fibroblasts on BrCa cells, fibroblasts (5×10^4) with indicated treatments were added into the upper chamber and MDA-231-LM2 cells (3×10^5) were added into the lower chamber of a 6-well cell culture insert with 0.4 μm pore size (Merk Millipore). These two cell types were co-cultured for 4 days followed by Western blot and migration assays.

Flow cytometry

To assay the expression of CCR4, 10^6 cells were incubated at room temperature for 30 min with 5 μl of non-specific isotype-matched control IgG and 5 μl of mouse monoclonal antibodies conjugated with PE fluorochrome (Cat. no. 12-1949; eBioscience). Unbound antibodies were removed by washing the cells twice in PBS buffer. Cells were subsequently analysed by multicolor flow cytometry using CellQuest software.

Tissue microarrays (TMA) and scoring

After IHC staining, the TMA chips of human BrCa clinical samples were digitally scanned by the Aperio Scanscope XT automated slide scanner, and the whole field of each tissue spot was obtained for IHC evaluation. The expression levels of epithelial HIC1, stromal CXCL14 and CCL17 were scored semiquantitatively based on staining intensity and distribution using the immunoreactive score (IRS). Briefly, Immunoreactive score (IRS) = SI (staining intensity) \times PP (percentage of positive cells). SI was assigned as: 0 = negative; 1 = weak; 2 = moderate; 3 = strong. PP is defined as 0 = 0%; 1 = 0-25%; 2 = 25-50%; 3 = 50-75%; 4 = 75-100%. For categorization of the continuous IRS values into low and high, we chose a cutoff point for the measurements (range 0-12, cut point ≤ 4 versus > 4).

Data mining

The *HIC1* mRNA expression of BrCa tissues were obtained from a TCGA dataset (TCGA_BRCA_exp_HiSeqV2-2015-02-24). The *CXCL14* mRNA expression of BrCa tissues were obtained from two Oncomine datasets (Finak Breast and Perou Breast) by Oncomine Cancer Microarray database analysis (<http://www.oncomine.org>). Then data were retrieved from the website and reanalyzed in GraphPad software. For analysis of the relationship between *HIC1* or *CCL17* mRNA expression and the RFS, OS and DMFS of BrCa patients, data were obtained from the Kaplan–Meier plotter database (<http://kmplot.com/analysis>) (5).

Supplementary References

1. Nair SJ, Zhang X, Chiang HC, Jahid MJ, Wang Y, Garza P, et al. Genetic suppression reveals DNA repair-independent antagonism between BRCA1 and COBRA1 in mammary gland development. *Nature communications*. 2016;7:10913.
2. Cheng G, Sun X, Wang J, Xiao G, Wang X, Fan X, et al. HIC1 silencing in triple-negative breast cancer drives progression through misregulation of LCN2. *Cancer research*. 2014;74(3):862-72.
3. Zhang HN, Yang L, Ling JY, Czajkowsky DM, Wang JF, Zhang XW, et al. Systematic identification of arsenic-binding proteins reveals that hexokinase-2 is inhibited by arsenic. *Proceedings of the National Academy of Sciences of the United States of America*. 2015;112(49):15084-9.
4. Myers SJ, Wong LM, and Charo IF. Signal transduction and ligand specificity of the human monocyte chemoattractant protein-1 receptor in transfected embryonic kidney cells. *The Journal of biological chemistry*. 1995;270(11):5786-92.
5. Gyorffy B, Lanczky A, Eklund AC, Denkert C, Budczies J, Li Q, et al. An online survival analysis tool to rapidly assess the effect of 22,277 genes on breast cancer prognosis using microarray data of 1,809 patients. *Breast cancer research and treatment*. 2010;123(3):725-31.